REVIEW OF RESEARCH
IMPACT FACTOR : 5.7631(UIF) UGC APPROVED JOURNAL NO. 48514 ISSN: 2249-894X
VOLUME - 8 | ISSUE - 2 | NOVEMBER - 2018

Review Article

CHARACTERIZATION TOOLS

R. K. Dhokale
Arts,Science and Commerce College,Naldurg, Dist.Osmanabad (MS) India.
Corresponding author: rkdhokale@gmail.com

ABSTRACT

The area of nanomaterials generally deals with experimental investigations and theoretical interpretation of the various physical as well as chemical properties of matter in nano scale. In the 21st century, the properties of materials at the nanoscales have become important from technological point of view and also have scope for their use in various fields such as electronics, biomedical, catalysis, computer technology, etc. Of course, among these allied areas, the ultimate goal of research in heterogeneous catalysis is to correlate the structure and composition of a catalyst with its performance. Catalyst performance is judged in terms of its activity, selectivity, reusability and ecofiendly nature. The characterization is one of the crucial aspects of catalyst-based process since it gives information about structural behaviour, crystalline phases, nature of active sites, particle size and morphology, acidity, and other characteristic features.

KEYWORDS: *X-ray, Electron Microscopy.*

INTRODUCTION :

X-ray Diffraction

X-ray diffraction (XRD) is a well-known technique for knowing the structural properties of the matter. Scientist V. Laue, in 1912, reasoned that incident X-rays are diffracted when wavelength of incident X-rays equal to the interatomic distance in crystals. At the beginning, the use of X-ray diffraction was very limited for the determination of crystal structure of simple compounds.

When a beam of X-rays having a single wavelength strikes the sample material, X-rays are scattered in all directions. Most of the radiation scattered from one atom cancels out the radiation scattered from other atoms. However, X-rays that strike certain crystallographic planes at specific angles are reinforced rather than annihilated. This phenomenon is called constructive interference or diffraction. The X-rays are diffracted, or the beam is reinforced, when the conditions satisfy Bragg's law,

$$n\lambda = 2d.\sin\theta \qquad \text{---------- 1}$$

Where, θ is half of the angle between the diffracted beam and the incoming beam, λ is the wavelength of the X-rays used, and dis the interplanar spacing between the planes that cause constructive interference of the beam [1-3].

Recently, this tool is applied not only for structural elucidation but also for the determination of orientation /quality of single crystals, phase diagrams, chemical analysis, grain size, strain/stress measurements, etc.[3]In the following section, we briefly outline some important applications of XRD-technique:

i) Calculation of crystallite size

The crystallite size of the samples was determined by Scherrer's formula given by

$$D = 0.9 \lambda / \beta \cos\theta \qquad \text{---------- 2}$$

where, λ is the wavelength of X-ray radiation used, β is full width at half maximum (FWHM) in radian and D is diameter of crystal particle.

ii) Determination of crystal structures

Nanocomposites can be identified by comparing its diffraction pattern with a standard diffraction pattern from ASTM or JCPDS database. In this case, the XRD data with respect to line positions (2θ degree) and intensities are examined. X-ray diffraction supplements data are used for determining the crystal structures of the various phases involved in the analyte. The key to interpret the powder pattern of an alloy is the fact that each phase produces its own pattern.

iii) Phase identification

The powder diffraction pattern of a nanocrystalline compound is a typical characteristic of that substance and forms a sort of fingerprint by which the substance may be identified. Diffraction pattern of a pure nanocrystalline material is given in the standard powder diffraction file. The usual way of identifying a substance is to match its observed diffraction pattern, both in angular position and the intensity with that of standard. The mixture of substances may be identified provided, the pattern of the component phases are available for comparison. Substances are indexed by one of the two methods. Hanawalt index method uses the eight most intense lines; while Fink index method uses the first eight lines, of longest *d*-spacing, in the powder pattern.

The quantitative analysis of a mixture become difficult when a line superimposed on a line from another and when this composite line is one of the three strongest lines in the pattern of the unknown. In such cases, an internal standard method is used to identify the phases. A line in the powder pattern of the phase of interest is selected and its intensity is compared with suitable internal standard line. The amount of phase present in the substance can be determined by interpolation from a previously constructed calibration graph of intensity versus compositions.

iv) Determination of unit cell parameters

The positions (d-spacing) of the lines in a powder pattern are governed by the values of the unit cell (*a, b, c, α, β, γ*). Unit cell parameters are normally determined by a single crystal method but the values obtained are often accurate to only two or three significant decimals. More accurate cell parameters may be obtained from powder pattern, provided the various lines have been assigned Miller indices '*hkl*' and their positions have been measured accurately. Using a least square minimization procedure, unit cells parameters accurate to four or five significant figures may usually be obtained. Accurate unit cell parameters are particularly useful for (a) enabling complex powder patterns to be indexed (b) studying the effects of composition on cell parameters and (c) measuring thermal coefficients.

There are several computer programs available for automatic determination of the unit cell parameters from the observed d-values.

v) Solid solution lattice parameters

The lattice parameters of solid solution series often show a small but detectable variation with composition. This provides a useful means of characterizing solid solutions and, in principle, lattice parameters may be used as an indicator of composition. If the composition dependence is linear then, the so-called, Vegard's Law is obeyed. This law often occurs in metallic solid solutions. In non-metallic solid solutions, deviations from Vegard's law are much less common and, when they occur, can usually be

ascribed to structural features in the solid solutions. More common, this law generalizes solid solution formation by either random substitution or distribution of ions.

vi) Crystallite size measurement and residual strain (extended formula)

X-ray powder diffraction is used to measure the average crystal size in a powdered sample, provided the average diameter is less than about 2000 Å. The lines in a powder diffraction pattern are of finite breadth but if the particles are very small the lines are broader than usual. When the size of the individual crystals is less than about 1 µm, the crystallite size is calculated from full width at half maximum (FWHM) using following relation for cubic and hexagonal phases; [5]

$$\beta_{2\theta}\cos\theta = (k.\lambda / D) + 4\varepsilon' \sin\theta \qquad \text{------- 3}$$

Where, $\beta_{2\theta}$ is the broadening of diffraction line measured at half of its maximum intensity (in radians), D is the diameter of crystal particles, λ is the wavelength of the X-ray used, k is the constant related to shape of the crystallites. It varies from 0.9-1.3. It is best approximated to a value of 0.9, when little is known about the crystallite size and shape. ε' is the residual strain of the films. A plot of $\beta_{2\theta}\cos\theta$ against $\sin\theta$ will give a straight line with intercept. The intercept and slope of the graph are related to the grain size and residual strain respectively.

vii) Intensity considerations

The X-ray intensities of diffracted beam depend on the position of the atoms in unit cell. This intensity calculation of diffracted beam is complex because of the many variables involved such as polarization factor, structure factor, multiplicity factor, Lorentz factor, absorption factor and temperature factor. The exact intensity equation of diffracted X-ray beam for the diffractometer is

$$I = F.\ p.\ [(1+\cos^2 2\theta)/(\sin^2\theta.\ \cos\theta)].e^{-2M} \qquad \text{---------- 4}$$

Where, the symbols used have their particular meanings.

viii) Short range order in crystalline solids

Non-crystalline solids give diffraction pattern that has a small number of very broad humps. From these humps, information on local structure may be obtained. The results are usually presented as a radical distribution function (RDF). This shows the probability of finding an atom as a function of distance from reference atom. Information is thereby obtained on coordination environments (first and outer spheres) and bond distances. Such information is useful for testing validity of structural models for non-crystalline.

ix) Crystal defects and disorder

Certain types of defects and disorder that occur in crystalline solids can be detected by a variety of diffraction effects. Generally, this property generalizes with the help of X-ray line broadening, strain within the crystal and temperature factor. This property causes a reduction in peak intensity and an increase in the level of background radiation.

In the present study, the XRD patterns of the supported metal nanoparticles were recorded on a Brucker make X-ray diffractometer (Model D8) with following specifications.

- Target used : Cu-Kα
- Scanning rate : 2° per minute
- Range of 2θ: 10° and 100°.

Transmission Electron Microscopy and Selected Area Electron Diffraction (TEM and SAED)

Electron microscopes use electrons instead of photons because the former have shorter wavelengths, allowing the observation of matter with atomic resolution. In a transmission electron microscope (TEM), electrons are shot through the sample, and changes in the electron beam arising from scattering by the sample are measured.

The morphological features of the nanocomposites were evaluated by TEM.Prior to TEM measurements, the samples were dispersed in suitable organic solvent like isoamyl acetate, acetone, toluene, etc, and a drop of the solution was poured on carbon-coated TEM grids. The film formed on the TEM grids was allowed to dry for 12 hours under high voltage lamp following which the extra solvent was removed using a blotting paper and the TEM measurements were performed. TEM operates on principles similar to that of the optical microscope [4]. The sample illumination source in a TEM is a beam of electrons. This beam of electrons goes through a column under vacuum and is then focused into a very narrow beam with electromagnetic lenses. Some electrons will scatter and those that do not scatter strike a fluorescent screen giving rise to a contrast image based on sample density. Since the limit of resolution is in the order of a few angstroms, it is a very useful and powerful tool for nanoparticle characterization. Low resolution TEM can generally provide information regarding the size and overall shape of the sample and is routinely used to elucidate such information. Moreover, it is highly useful for determination of the lattice planes and the detection of atomic-scale defects in areas of few nanometers in diameter with the help of selected area electron diffraction (SAED) technique. SAED patterns obtained by TEM providing the information related to the orientations, atomic arrangements, and structures of narrow regions of interest in NMs. Energy electron loss (EEL) phenomenon in TEM, which makes use of the inelastic scattering of the incident electrons on the sample, is an important tool for qualitative and quantitative analysis of elements.

In the present studies, TEM images of the samples were recorded on a Tecnai F30 field emission transmission electron microscope operating at 300 kV. Selected area electron diffraction (SAED) images were also recorded.

Scanning Electron Microscopy (SEM)

In the present studies, scanning electron microscopy (SEM) micrographs of the representative samples were obtained using scanning electron microscope (Model: JEOL JSM 6360) (Fig. 1).

At one extreme, SEM complements optical microscopy for studying the texture, topography and surface features of powders or solid pieces, because of the depth of focus of SEM instruments, the resulting pictures have a definite three-dimensional quality. At the other extreme, high resolution scanning electron microscope (HREM) or field-emission scanning electron microscope (FE-SEM) is capable of giving information on atomic scale by direct lattice imaging. The resolution of ~ 2 Å has been achieved [5-7].

The grain size of the sample was calculated by Cottrell's method which gives relation between the number of intercepts of grain boundary per unit length (P_L) and total number of intercepts (n) as.

$$P_L = (n/2\pi r)\, M \qquad \text{---------- 5}$$

where M is the magnification at which SEM micrograph is scanned, 'r' is radius of circle and n is the number of grains in the circle. Using equation 3.8 the grain diameter (L) can be calculated as,

$$L = 1/P_L - 1 \qquad \text{---------- 6}$$

This equation gives the average grain diameter.

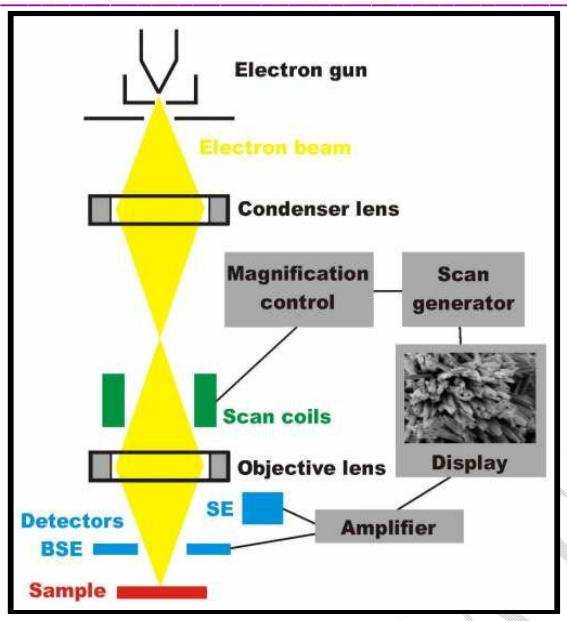

Fig.1: Schematic diagram of Scanning Electron Microscope

Energy dispersive X-ray atomic spectroscopy (EDAX)

Energy-dispersive X-ray atomic spectroscopy (EDAX) is used mainly for elemental analysis and for chemical characterization of samples [7]. The technique is based on the fact that every element has a unique atomic structure such that X-rays characteristic of different atomic structures are readily distinguishable from one another. In EDAX, the incident electron beam excites an electron in an inner shell, causing its ejection and the formation of an electron hole in the electronic structure of the atom. An electron from a higher-energy (outer) shell fills the hole, and the energy difference between the higher-energy shell and the lower-energy shell is released as X-rays. The X-rays thus released are analyzed by means of an energy-dispersive spectrometer. EDAX systems are associated with SEM and TEM.

There are four primary components of the EDAX setup: the beam source; the X-ray detector; the pulse processor; and the analyzer. Scanning electron microscopes, which are equipped with a cathode and magnetic lenses to create and focus a beam of electrons; a detector is used to convert X-ray energy into voltage signals; pulse processor and an analyzer for data display and analysis.

Its characterization capabilities are due in large part to the fundamental principle that each element has a unique atomic structure allowing unique set of peaks on its X-ray spectrum. In order to stimulate emission of characteristic X-rays from a specimen, a high-energy beam of charged particles such as electrons or protons or a X-rays beam is focused into the sample under investigation. Initially, an atom within the sample contains ground state (or unexcited) electrons in discrete energy levels or electron shells bound to the nucleus. The incident beam may excite an electron in an inner shell, and create an electron hole by ejecting electron from the shell. An outer electron from higher-energy shell fills the electron hole, and the energy difference between the higher-energy shell and the lower energy shell may be released in the form of an X-ray. The number and energy of the X-rays emitted from a specimen can be measured by an energy-dispersive spectrometer. As the energy of the X-rays are characteristic of the difference in energy between the two shells, and of the atomic structure of the element from which they were emitted, this allows the elemental composition of the specimen to be measured.

Atomic Absorption Spectroscopy (AAS)

The principle of atomic absorption is based on energy absorbed during transitions between electronic energy levels of an atom. On providing some kind of energy to an atom in ground state by means

of a flame (temperature range 2200–2400°C), outer-shell electrons are promoted to a higher energy excited state. The radiation absorbed becaus of the transition between electronic levels can be used for quantitative analysis of metals present in solid matrices, which have to be dissolved in proper solvents before analysis. The quantitative analysis depends on measurement of radiation intensity and the assumption that radiation absorbed is proportional to atomic concentration. Analogy of relative intensity values for reference standards is used to determine elemental concentrations [8].

Atomic absorption spectroscopy (AAS) was used for compositional analysis of the metals in the nanocomposites. The metal nanocomposite was treated with concentrated AR grade HNO_3. This solution was used for quantitative analysis by Perkin Elmer (USA) 3030 atomic absorption spectrometer following a standard method. The instrument was calibrated to zero absorbance for aqueous solutions of known concentrations [9, 10].

The calibration curve is produced. In case of high concentrated solutions this curve is rescaled. The more concentrated solutions absorb more radiation up to a specific absorbance. The calibration curve shows the concentration against the amount of radiation absorbed. The calibration curve was used to determine the unknown concentration of an element in a solution. The instrument was calibrated using several solutions of known concentrations. The absorbance of each known solution was measured and then the calibration curve of concentration against absorbance was plotted. The sample solution was fed into the instrument, to measure the absorbance of the element in this solution. The unknown concentration of the element was calculated from the calibration curve.

Photoluminescence (PL)

The photoluminescence (PL) measurements were done with an instrument Spectrofluorimeter (JASCO FP-750) with a 150W xenon lamp with shielded lamphouse lamp as the excitation source and silicon photodiode for Ex. monochromator and Photomultiplier tube for Em. monochromator detector. The emission spectra were recorded with a resolution of 1.0 nm, by exciting the samples at 325 nm. All the emission patterns were corrected for the detector response and were measured at 1 nm resolution.

The Spectrofluorimeter (JASCO FP-750) is shown in the form of schematic diagram in Fig. 2. The light is incident on the monitoring detector (Silicon photodiode) emission detector (PMT) which converts into an electrical signal, which is converted into digital signal by the A/D converter and is introduced to the computer. The signal subjected to arithmetic operation by the computer is outputted to the display unit as digital data or spectrum. Both wavelength as well as slit drives is controlled by the computer [11].

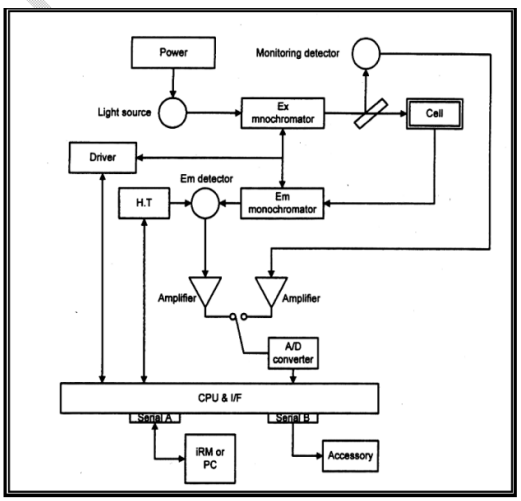

Fig.2: Schematic diagram of spectrofluorimeter.

LS: Light source (150W xenon lamp)	M2,M5,M6 : Plane mirror
M1: Ellipsoidal mirror	M3, M4 : Ellipsoidal entrance/ exit slit
S1: Excitation entrance/exit slit	S2: Emission entrance/exit slit
G1: Excitation concave diffraction grating (1200lines/mm)	G2: Emission concave diffraction grating (1200lines/mm)
SP: Silicon photodiode PMT: Photomultiplier tube	BS : Beam splitter MO,M7: Spherical mirror

Fourier Transform Infrared Spectroscopy (FTIR)

The interaction of probe molecule with atoms or molecules on the surfaces, either in the bulk form or physisorbed or chemisorbed form is of fundamental importance in nano-scale heterogeneous catalysis. FTIR is very versatile tool to investigate the mechanics & kinetics of such interactions. This technique deals with the vibrational & rotational levels in the molecules. The infrared region of the electromagnetic spectrum encompasses radiation with wavelengths ranging from 1 - 1000 microns. This range is divided into three regions; near IR (12500–4000 cm^{-1}), mid IR (4000–200 cm^{-1}) & far IR (200–10 cm^{-1}). The majority of analytical applications are confined to a portion of the infrared region originate for transitions between vibrational & rotational levels of a molecules present in its ground electronic state. Though, the absorption of far infrared radiations does result in a change of rotational energy, the pure rotational spectra are observed only with gases. In liquids & solids the rotational states are no longer well defined & affect the spectra of condensed phase only in terms of broadening of the vibrational bands [12]. The atoms in a molecule are never stationary & it is a good approximation to treat them as a combination of point masses held together by Hooks law of forces. By classical mechanics it can be shown that the displacement of the masses due to a particular set of vibrations. If in these set of vibrations the masses are in phase & the motion of all the nuclei involved in such that the center of gravity of the molecule remains unaltered then such vibrations are known as the fundamental modes of the molecule. Most of the time, a normal mode is localized largely to a group with in the molecule & hence corresponding to stretching or bending of one or few bonds only & hence associated with that particular functional group. Whether for the functional group or the entire molecule, the vibrations are universally classified either stretching or bending types. As stretching which corresponds to the oscillations leading to change bond lengths can be further subdivided in to symmetric or asymmetric stretching vibration. Bending vibrations are characterized by continuously changing the angle between the bonds & is further sub classified as wagging, rocking, twisting, and scissoring.Hooks law as presented below can calculate frequency of these vibrations,

$$\upsilon = 1/2\pi[K(m_1+m_2)/m_1.m_2]^{1/2}$$

$$\text{OR} \quad \upsilon = 1/2\pi[K/\mu]^{1/2} \qquad \ldots\ldots\ldots\ldots(7)$$

Where K the reduced mass & m_1, m_2 are the reduced masses of the atoms concerned in gram in particular bond & relates to the strength of the bond.

FTIR spectra of the NPs were recorded on BRUKER Alpha FT-Infra-Red spectrometer in the range of 400 cm^{-1} – 4000 cm^{-1} in the transmission mode.

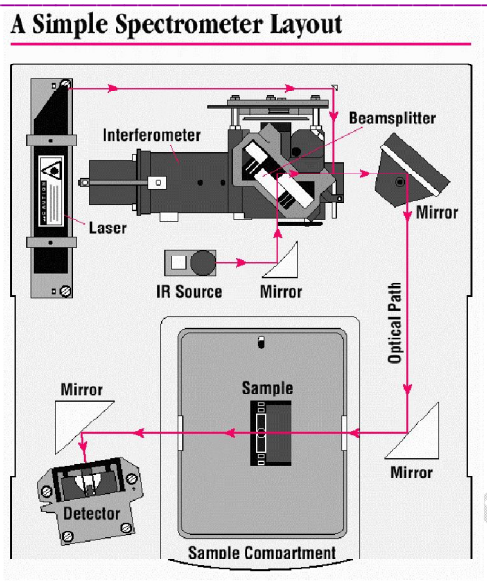

Fig. 3: FT-IR Spectrometer.

UV-VIS Spectroscopy (UV-Vis)

UV-Visible spectroscopy involves measuring the attenuation of a beam of light after it passes through a sample or after it is reflected from the sample surface [5,6]. This attenuation may arise from absorption, scattering, reflection, or interference. The simplest optical measurements are transmission (absorption) and reflectivity. For transmission measurements in wavelengths ranging from 150 nm (ultraviolet) to 3000 nm (near-infrared), commercially available dual-beam spectrophotometers may be used. One can obtain information about the size and shape of metal nanocrystals by measuring the position and nature of the surface plasmon absorption bands in the UV-visible region. In the case of semiconducting nanocrystals, optical measurement is the most important way of determining the band structure of semiconductors. The band gap is the fundamental property of semiconductors which is the energy separation between the filled valance band and the empty conduction band. The absorption of radiation in a material is considered to be due to inner shell electrons, valence band electrons, free carriers and electron bound to localized impurity centers or defects of some type. Optical excitation of electrons across the band gap is strongly allowed, producing an sudden increase in absorptivity at the wavelength corresponding to the gap energy. This feature in the optical spectrum is known as the optical absorption edge. For those structures with band gaps in the range of 0.3 to 3 eV, the optical absorption edge can be easily measured by conventional UV-Visible spectroscopy.

In order to obtain the UV-Vis spectra, the wavelength of maximum absorption must be measured. The sample solutions are placed in a quartz cells. Most of the spectrophotometers are double beam. The primary source of light splits into two beams, one passes through a cell containing the sample and other through the reference cell. The detector measures the intensity ratio of the reference beam with the sample beam.

The principle behind is the Lambert's- Beer's law which is formulated as

$$\varepsilon = A/cl \qquad \text{.....(8)}$$

Where, c is the molar concentration of an analyte, A is absorbance and ε is molar extinction coefficient.

Metal NPs exhibit the absorption of visible electromagnetic waves by the collective oscillation of conduction electrons at the surface known as the surface plasmon resonance effect. The interest in this

effect is the possibility of using it as a tracer for the presence of metal NPs with a simple UV-visible spectrophotometer.

In the present investigation, the UV-Visible spectra of all the samples were recorded in the range of 250-800 nm, using Perkin-Elmer Lambda 750 model. The samples were dispersed in solvent.

Magnetic measurements: B-H Loop Tracer

Magnetic characterization of nanomaterials (NMs) was generally carried out using a high field hysteresis loop tracer designed by Tata Institute of Fundamental Research, Mumbai (Fig 3.4). The main parts of the hysteresis loop tracer are, i) Electromagnet, ii) Pickup coil system, iii) Balancing and integrating network, iv) Preamplifier.

High magnetic field is generated in a solenoid by passing a pulse current of sinusoidal shape. In the solenoid, pickup coil system is kept to detect field and magnetization signal of a sample placed in the pickup coil. The signals produced are then processed by an electronic system. These transitory signals are digitized by micro-controller and then sent to computer for plotting a hysteresis loop which is observed on the monitor with calculated values of hysteresis parameters. These can be printed or stored as files. The system is useful for samples in powder or pallet form.

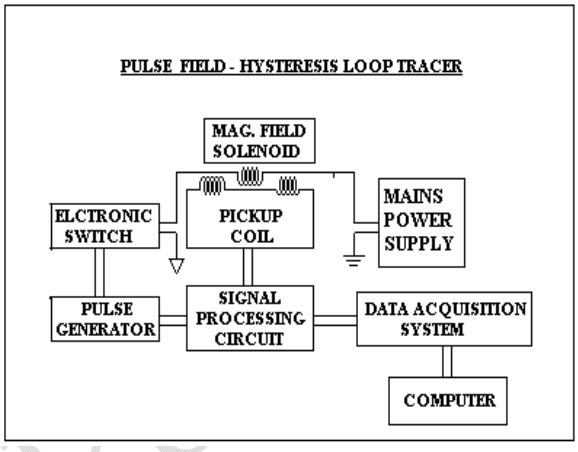

Fig. 4: Schematic diagram of the Hysteresis loop Tracer

The two C cores (English Electric Co-type WR/110/32/ 13) of laminated grain oriented silicon steel with cross section of the holes 5 x 2.5 cm have been used for this purpose. From one of C cores were joined together. The energizing coil for the magnet consists of 2200 turns of 20 swg super enamelled copper wire (resistance 11.5 ohms) wound on a perspex former and held together on the wooden base.

A multicoil which can be introduced in the pole gap serves as a pick up coil system. It consists of different windings, one over the other, wound with 39 swg super enamelled copper wire on a Perspex former. A multicoil is connected through the balancing and integrating network to the amplifier and then to the y plates of the oscilloscope. The input of the x plate is taken from the emf developed across a resistance connected in series with proper inductance and variable resistance. The multiple units were slid into the pole gap and current in the energizing coil was increased to produce the required field.

The potentiometer and variable resistance in the balancing network were adjusted to get a horizontal trace on the oscilloscope. After reducing the current to zero; the multicoil was pulled out and the sample pellet kept at the central gap in the multicoil spool and introduced into the pole gap. The current in the energizing coil was raised to a sufficient value till the sample saturates. The hysteresis loop produced on the oscilloscope was recorded for the accurate measurement of magnetization.

When the particle size is very small (<10–15 nm), the particles become superparamagnetic. Nanocrystals of many materials show evidence of the presence of ferromagnetic interactions at low temperatures. This is especially true of nanocrystals of antiferromagnetic oxides such as MnO, CoO, and NiO. Room-temperature ferromagnetism has been observed even in nanocrystals of nonmagnetic materials, including CeO_2, Al_2O_3, ZnO, In_2O_3, SnO_2, GaN, and CdS. All of these materials showed characteristic magnetic hysteresis that was not found in the bulk samples. Given that no magnetic impurities were present, the origin of ferromagnetism may be the exchange interactions between the localized electron spin moments that result from anion or cation vacancies at the surfaces of nanocrystals. Thus, ferromagnetism or paramagnetism may indeed be a universal characteristic of nanocrystals [13, 14].

Nuclear magnetic resonance spectroscopy (NMR) techniques

^1H NMR spectra were recorded on a Brüker 400 MHz NMR spectrometer in $CDCl_3$ at room temperature (25 ^oC). Nuclear magnetic resonance (NMR), is a phenomenon which occurs when the nuclei of certain atoms are immersed in a static magnetic field and exposed to a second oscillating magnetic field. Some nuclei experience this phenomenon, and others do not, dependent upon whether they possess a property called spin. The water molecule having one oxygen and two hydrogen atoms. Thus, we zooming into one of the hydrogen's past the electron cloud we observe a nucleus with single proton. The proton possesses a property called spin which:

I) Can be thought as an small magnetic field, and II) It will cause the nucleus to produce an NMR signal. Not all nuclei possess the property called spin.

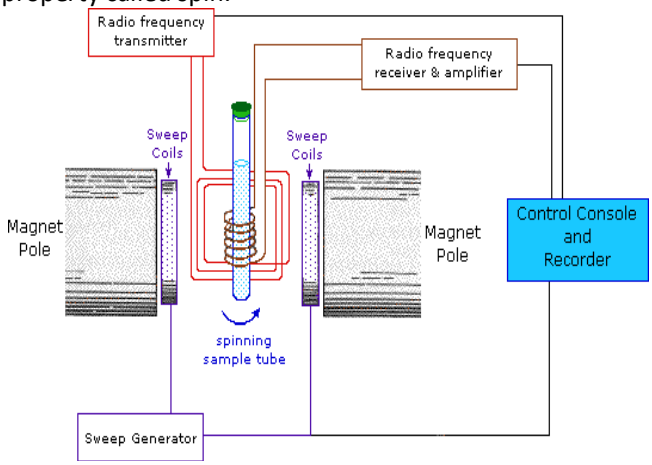

Fig. 5: Schemtaicreprsentation of the NMR Spectrophotometer.

Chemical Shift

When an atom is placed in a magnetic field, its electrons circulate about the direction of the applied magnetic field. This circulation causes a small magnetic field at the nucleus which opposes the externally applied field. The magnetic field at the nucleus (the effective field) is therefore generally less than the applied field by a fraction. In some cases, such as the benzene molecule, the circulation of the electrons in the aromatic orbitals creates a magnetic field at the hydrogen nuclei which enhances the B_o field. This phenomenon is called deshielding. In this example, the B_o field is applied perpendicular to the plane of the molecule. The ring current is traveling clockwise if you look down at the plane. The electron density around each nucleus in a molecule varies according to the types of nuclei and bonds withinmolecule. The opposing field and effective field at each nucleus will vary. This is called the chemical shift. The chemical shift of a nucleus is the difference between the resonance frequency of the nucleus and a standard, relative to the standard. This quantity is reported in ppm and given the symbol delta, In NMR spectroscopy, this standard is

often tetramethylsilane, $Si(CH_3)_4$, abbreviated TMS. The magnitude of the screening depends on the atom. For example, carbon-13 chemical shifts are much greater than hydrogen-1 chemical shifts.

Spin-Spin Coupling

Nuclei experiencing the same chemical environment or chemical shift are called equivalent. Those nuclei which possesing different environment or having different chemical shifts is nonequivalent. The Nuclei which are close to each other they exert an influence on each other's effective magnetic field. This effect was observed in the NMR spectrum, if the nuclei are nonequivalent. Thus, the distance is less then or equal to three bond lengths between non-equivalent nuclei is less than or equal to three bond lengths, then effect is observable, such effect is called spin-spin coupling or *J* coupling.

Configuration	Peak Ratios
A	1
AB	1:1
AB_2	1:2:1
AB_3	1:3:3:1
AB_4	1:4:6:4:1
AB_5	1:5:10:10:5:1
AB_6	1:6:15:20:15:6:1

Above figure represent Pascal's triangle and can be calculated from the coefficients of the expansion of the equation [15,16].

CONCLUSION

X-ray powder diffraction is used to measure the average crystal size in a powdered sample, provided the average diameter is less than about 2000 A. The lines in a powder diffraction pattern are of finite breadth but if the particles are very small the lines are broader than usual.

In a transmission electron microscope, electrons are shot through the sample, and changes in the electron beam arising from scattering by the sample are measured.

SAED patterns obtained by TEM providing the information related to the orientations, atomic arrangements, and structures of narrow regions of interest in NMs. Energy electron loss phenomenon in TEM, which makes use of the inelastic scattering of the incident electrons on the sample, is an important tool for qualitative and quantitative analysis of elements.

In EDAX, the incident electron beam excites an electron in an inner shell, causing its ejection and the formation of an electron hole in the electronic structure of the atom.

The incident beam may excite an electron in an inner shell, and create an electron hole by ejecting electron from the shell.

REFERENCES

1. B.D. Culity, Elements of X-ray Diffraction, A. W. Publishing Co. Inc., (2nd eds.) (1978).
2. C.W. Whiston, X-ray Method, John Wiley, New York, (1991).
3. E. Lifsin, X-ray Characterization of Materials, John Wiley, New York, (1999) 37.
4. M. De Graef, Introduction to Conventional Transmission Electron Microscopy; Cambridge University Press: Melbourne, (2003)
5. N. J Hoboken, E.N. Kaufmann, Characterization of Materials, Eds. 2 vol. Wiley, (2003).
6. M. Hosokawa, K. Nogi, N. Naito, T. Yokoyama, Nanostructure and Function (Characterization of Local Nanostructure) in Nanoparticle Technology Handbook, Amsterdam: Elsevier. 1st Eds. (2007).
7. J. Goldstein, D. Newbury, D. Joy, C. Lyman, P. Echlin, Scanning Electron Microscopy and X-Ray Microanalysis, 3rd Eds. New York, Springer, (2003).

8. J. W. Robinson, Atomic Absorption Spectroscopy, Marcel Dekker, New York, (1975).
9. J. W. Robinson, Analytical Chemistry, 32 (1960) 17.
10. R. Matsuda, Y. Hayashi, K. Sasaki, Y. Saito, Analytical Chemistry, 70 (1998) 319.
11. J.R. Lakowicz, Principles of Fluorescence Spectroscopy, Plenum Press, New York, (1983).
12. Skoog, Principles of Instrumental Analysis, 3rdEds, Saunders Golden Sunburst Series, Ornaldo, (1985).
13. Sundaresan, R. Bhargavi, N. Rangarajan, U. Siddesh, C. N. R. Rao, Physical Review B, 74 (2006) 161306.
14. Madhu, A. Sundaresan, C. N. R. Rao, Physical Review B, 77 (2008)201306.
15. K.C. Wong, Journal of Chemistry Education, 91(2014) 1103.
16. P.S. Kalsi, Spectroscopy of Organic Compounds, The Sixth Edition, New Age International, (2007) p.652.